Electronic Supplementary Material (ESI) for Journal of Materials Chemistry A.

Revitalizing Spherical Au@Pd Nanoparticles with Controlled Surface-Defect Density as High Performance Electrocatalysts

Peina Zhang,[†] Yujiao Xiahou,[†] Jin Wang,[†] Lihui Hang,[¶] Dayang Wang[‡] and Haibing Xia,[*,†]

[†]State Key Laboratory of Crystal Materials, Shandong University, Jinan, 250100, P. R China;

[¶]School of Environmental Science and Engineering, Shandong University, Jinan, 250100, P. R China;

[‡]Department of Civil, Environmental and Chemical Engineering, School of Engineering, RMIT University, Melbourne, VIC 3001, Australia.

Fig. S1 TEM images of as-prepared Au NPs obtained by citrate reduction of $HAuCl_4$: 6.1 ± 1 nm (a), 12.1 ± 2 nm (b), 19.3 ± 2 nm (c), 30.4 ± 2 nm (d), and 57.2 ± 5 nm (e). Insets are the high-magnification TEM images of corresponding Au NPs.

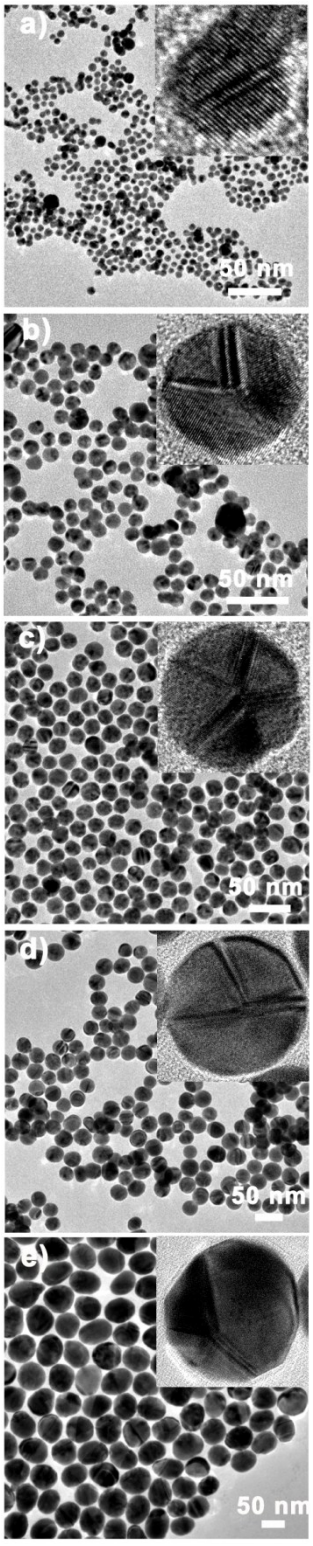

Fig. S2 Scanning transmission electron microscope—energy dispersive spectrometer (STEM-EDS) mapping image of 19 nm Au-NP seed.

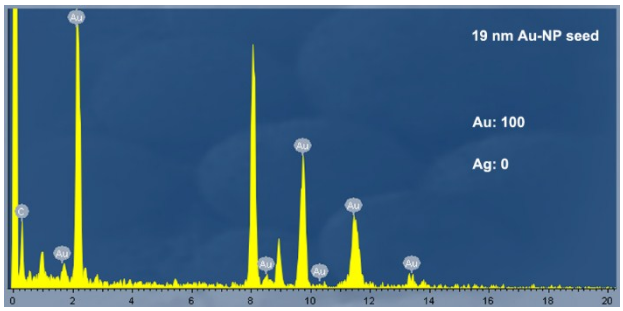

Fig. S3 TEM images (a-f) of $C_{19}S$ $Au_{0.91}@Pd_{0.09}$ NPs obtained by varying the additional amount of AA and their corresponding extinction spectra (g): 0 mM (a, blank curve), 0.04 mM (b, red curve), 0.4 mM (c, blue curve), 2 mM (d, olive curve), 4 mM (e, navy curve), and 8 mM (f, violet curve). The number of Au seed is 1.3×10^{12}. The concentrations of citrate and Na_2PdCl_4 are 4.12 and 0.02 mM, respectively. The Pd-to-Au molar ratio is 1:10.

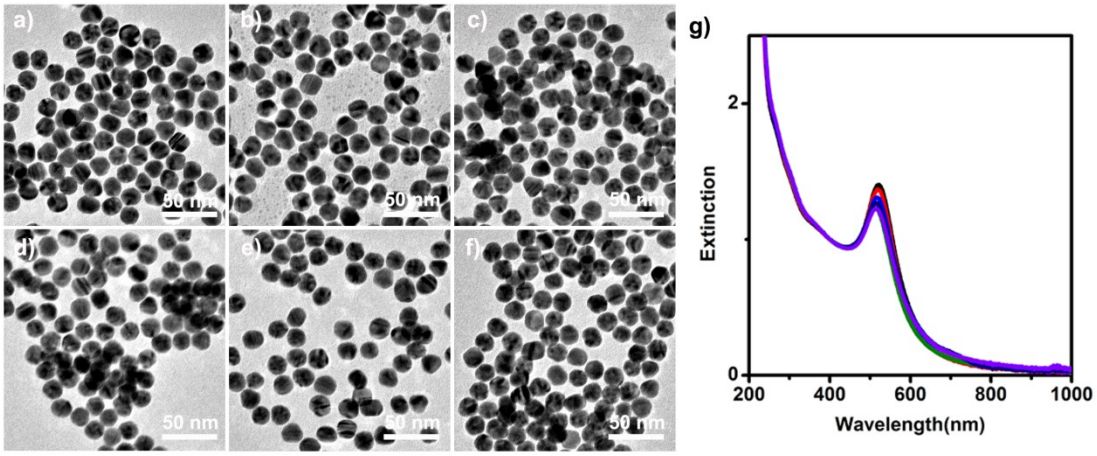

Fig. S4 CV curves (A and B) of GCEs modified by $C_{19}S$ $Au_{0.91}@Pd_{0.09}$ NPs obtained by varying the additional amount of AA measured in 0.50 M KOH solution in the absence (A) and presence (B) of 0.5 M ethanol: 0 mM (a), 0.04 mM (b), 0.4 mM (c), 2 mM (d), 4 mM (e), and 8 mM (f). The currents are normalized by the Pd mass loaded on the GCE. The scan rates are 50 mV s^{-1}. The number of Au-NP seeds is 1.3 × 10^{12}. The concentrations of citrate and Na_2PdCl_4 are 4.12 and 0.02 mM, respectively. The Pd-to-Au molar ratio is 1:10.

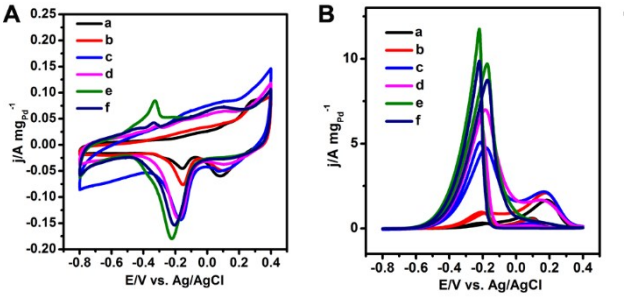

Fig. S5 HRTEM images of 19 nm Au-NP seed (a) and $C_{19}S$ $Au_{0.91}@Pd_{0.09}$ NP (b), and cross-sectional compositional line profile (c) of a $C_{19}S$ $Au_{0.91}@Pd_{0.09}$ NP.

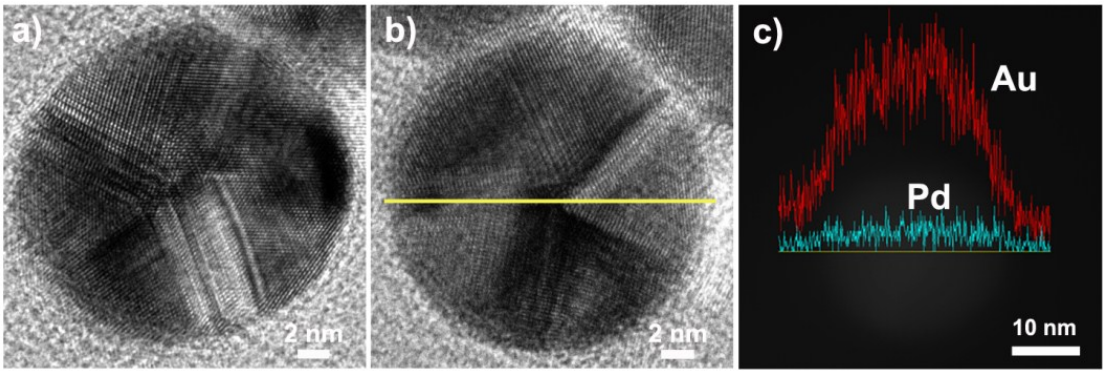

Fig. S6 XPS spectra of the Pd 3d signals (A) of pure Pd NPs and $C_{19}S$ $Au_{0.91}@Pd_{0.09}$ NPs, and XPS spectra of the Au 4f signals (B) of spherical pure Au NPs and $C_{19}S$ $Au_{0.91}@Pd_{0.09}$ NPs.

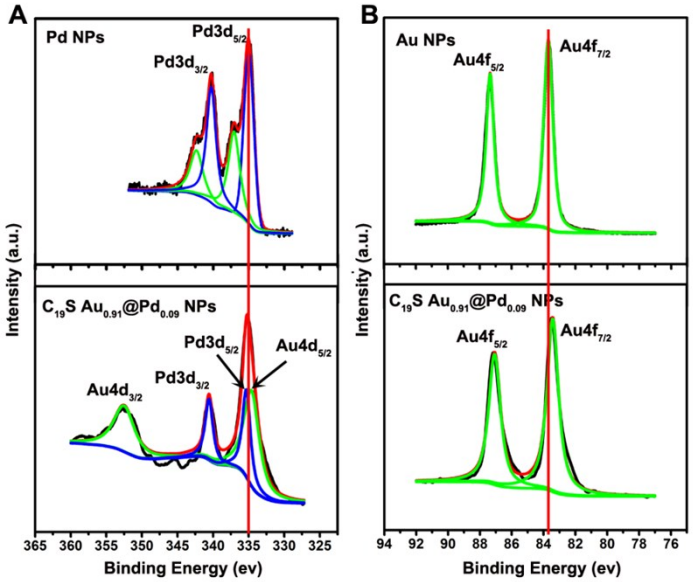

Fig. S7 Additional HRTEM images of as-prepared C_mS $Au_x@Pd_{1-x}$ NPs with various core sizes and about one Pd atomic layer: C_6S $Au_{0.76}@Pd_{0.24}$ NPs (A), $C_{12}S$ $Au_{0.85}@Pd_{0.15}$ NPs (B), $C_{19}S$ $Au_{0.91}@Pd_{0.09}$ NPs (C), $C_{30}S$ $Au_{0.95}@Pd_{0.05}$ NPs (D), and $C_{57}S$ $Au_{0.97}@Pd_{0.03}$ NPs (E), respectively.

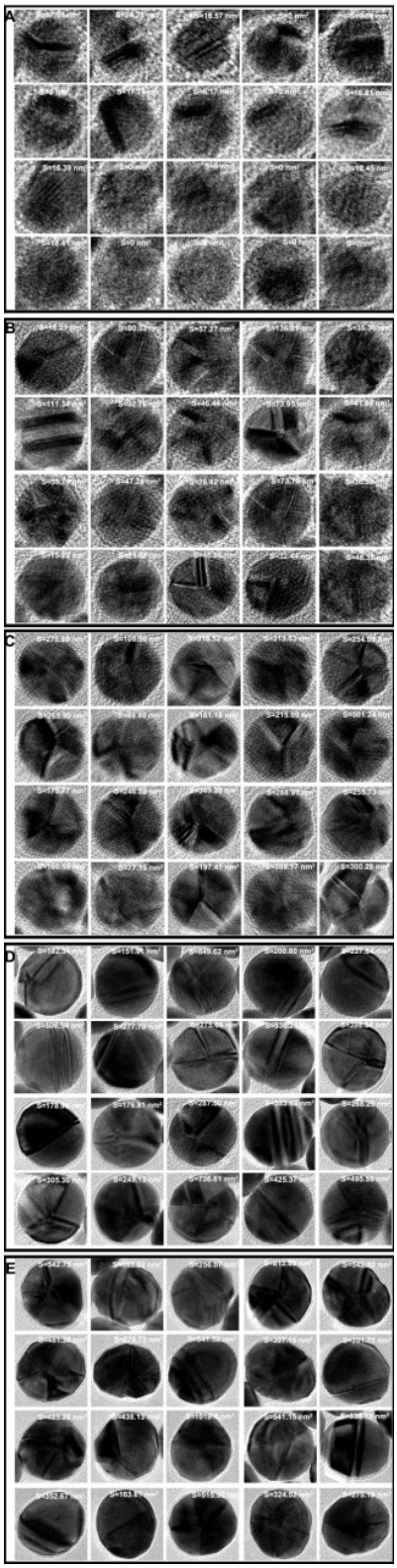

Fig. S8 TEM images of C_mS $Au_x@Pd_{1-x}$ NPs with carbon supports (a to e): C_6S $Au_{0.76}@Pd_{0.24}/C$ (a), $C_{12}S$ $Au_{0.85}@Pd_{0.15}/C$ (b), $C_{19}S$ $Au_{0.91}@Pd_{0.09}/C$ (c), $C_{30}S$ $Au_{0.95}@Pd_{0.05}/C$ (d), and $C_{57}S$ $Au_{0.97}@Pd_{0.03}/C$ (e), respectively.

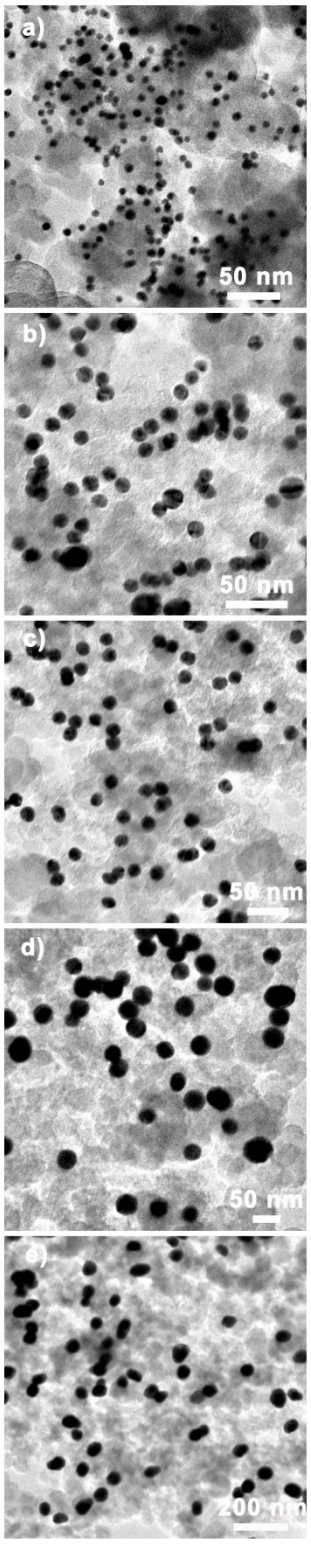

Fig. S9 CV curves (A–C) and CA curves (D) of the GCEs modified by C_6S $Au_{0.76}@Pd_{0.24}/C$ (a, black curve), $C_{12}S$ $Au_{0.85}@Pd_{0.15}/C$ (b, red curve), $C_{19}S$ $Au_{0.91}@Pd_{0.09}/C$ (c, blue curve), $C_{30}S$ $Au_{0.95}@Pd_{0.05}/C$ (d, magenta curve), $C_{57}S$ $Au_{0.97}@Pd_{0.03}/C$ (e, olive curve), and commercial Pd/C catalyst (f, navy curve), respectively, measured in 0.50 M KOH solution in the absence (A) and presence (B to D) of 0.5 M ethanol. The scan rates in panels A and D and panels B and C are 50 and 20 mV s^{-1}, respectively. The current densities are normalized by the Pd mass loaded (A, B, and D) and the ECSA values (C), respectively.

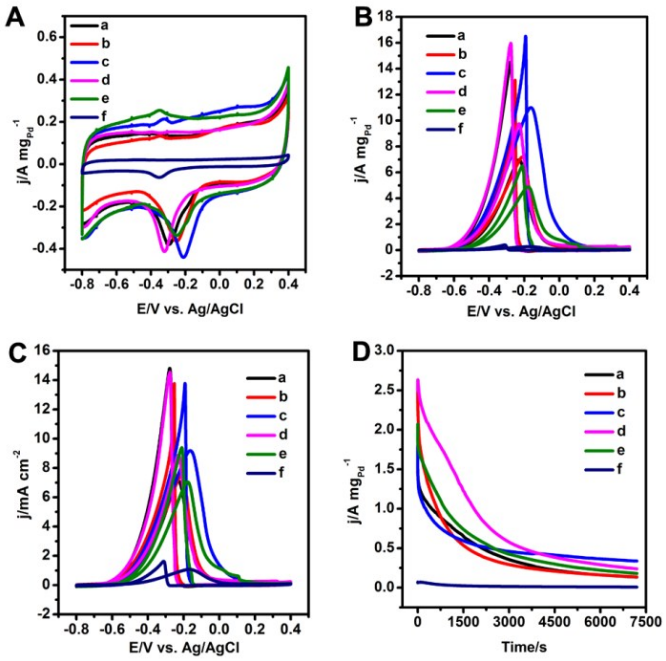

Fig. S10 CV curves (A–C) and CA curves (D) of GCEs modified by C_6S $Au_{0.76}@Pd_{0.24}$ NPs (a, black curve), C_6S $Au_{0.76}@Pd_{0.24}/C$ (b, red curve), and Pd/C catalyst (c, blue curve) measured in 0.50 M KOH solution in the absence (A) and presence (B to D) of 0.5 M ethanol. The scan rates in panels A and D and panels B and C are 50 and 20 mV s^{-1}, respectively. The current densities are normalized by the Pd mass loaded (A, B, and D) and the ECSA values (C). The concentrations of citrate, AA, Na_2PdCl_4 and Au-NP seeds are 4.12 mM, 4.0 mM, 0.02 mM, and 1.3×10^{13}.

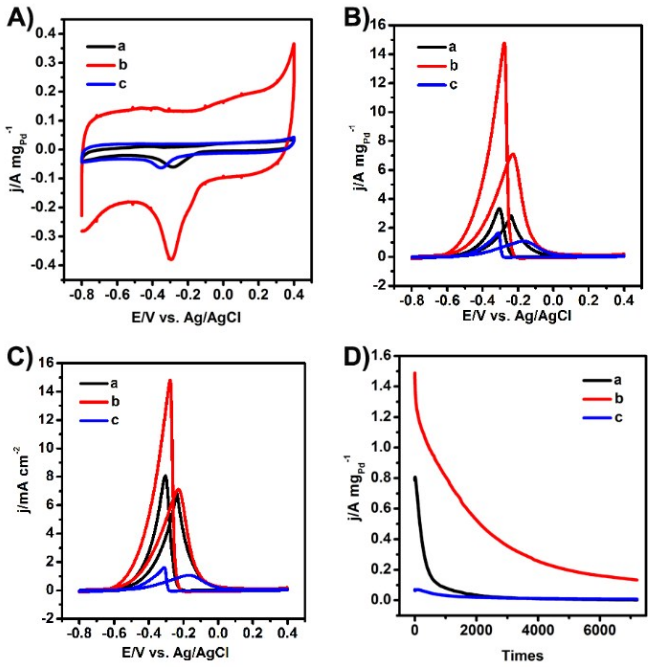

Fig. S11 CV curves (A–C) and CA curves (D) of GCEs modified by $C_{12}S$ $Au_{0.85}@Pd_{0.15}$ NPs (a, black curve), $C_{12}S$ $Au_{0.85}@Pd_{0.15}$ /C (b, red curve), and Pd/C catalyst (c, blue curve) measured in 0.50 M KOH solution in the absence (A) and presence (B to D) of 0.5 M ethanol. The scan rates in panels A and D and panels B and C are 50 and 20 mV s^{-1}, respectively. The current densities are normalized by the Pd mass loaded (A, B, and D) and the ECSA values (C). The concentrations of citrate, AA, Na_2PdCl_4, and Au-NP seeds are 4.12 mM, 4.0 mM, 0.02 mM, and 3.3×10^{12}.

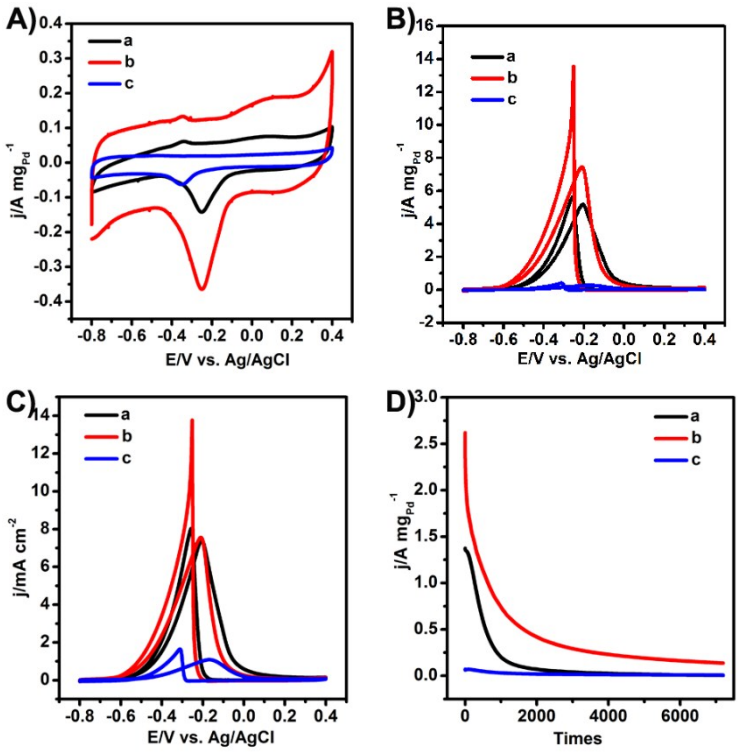

Fig. S12 CV curves (A–C) and CA curves (D) of GCEs modified by $C_{19}S$ $Au_{0.91}@Pd_{0.09}$ NPs (a, black curve), $C_{19}S$ $Au_{0.91}@Pd_{0.09}$ /C (b, red curve), and Pd/C catalyst (c, blue curve) measured in 0.50 M KOH solution in the absence (A) and presence (B to D) of 0.5 M ethanol. The scan rates in panels A and D and panels B and C are 50 and 20 mV s^{-1}, respectively. The current densities are normalized by the Pd mass loaded (A, B, and D) and the ECSA values (C). The concentrations of citrate, AA, Na_2PdCl_4, and Au-NP seeds are 4.12 mM, 4.0 mM, 0.02 mM, and 1.3×10^{12}.

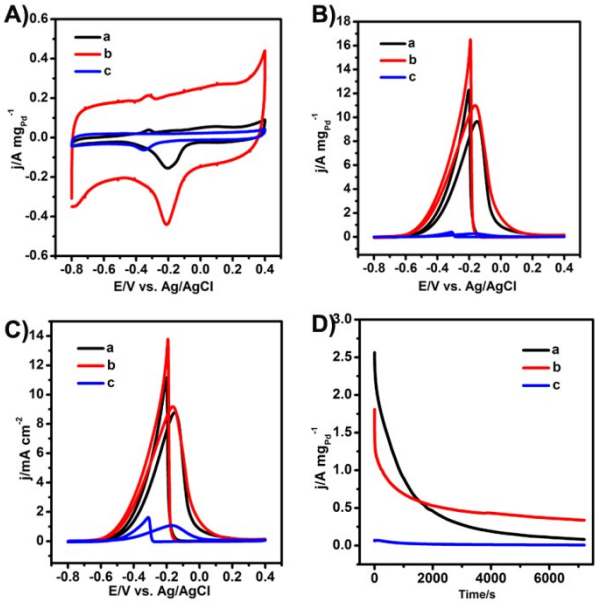

Fig. S13 CV curves (A–C) and CA curves (D) of GCEs modified by $C_{30}S$ $Au_{0.95}@Pd_{0.05}$ NPs (a, black curve), $C_{30}S$ $Au_{0.95}@Pd_{0.05}/C$ (b, red curve), and Pd/C catalyst (c, blue curve) measured in 0.50 M KOH solution in the absence (A) and presence (B to D) of 0.5 M ethanol. The scan rates in panels A and D and panels B and C are 50 and 20 mV s^{-1}, respectively. The current densities are normalized by the Pd mass loaded (A, B, and D) and the ECSA values (C). The concentrations of citrate, AA, Na_2PdCl_4, and Au-NP seeds are 4.12 mM, 4.0 mM, 0.02 mM, and 5.3×10^{11}.

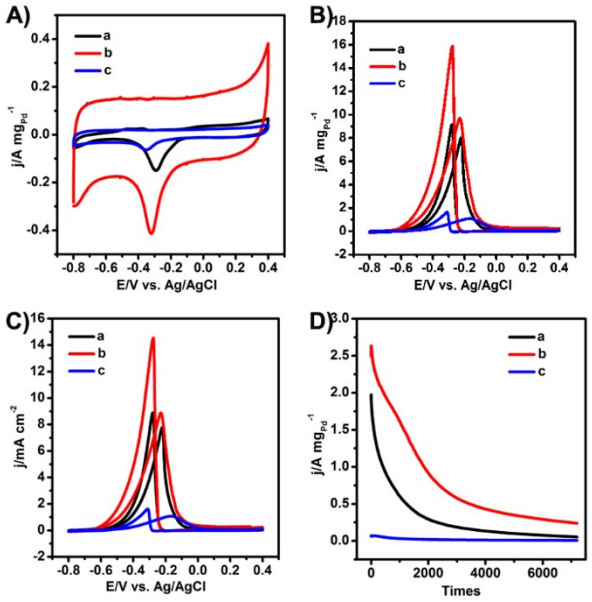

Fig. S14 CV curves (A–C) and CA curves (D) of GCEs modified by $C_{57}S$ $Au_{0.97}@Pd_{0.03}$ NPs (a, black curve), $C_{57}S$ $Au_{0.97}@Pd_{0.03}$/C (b, red curve), and Pd/C catalyst (c, blue curve) measured in 0.50 M KOH solution in the absence (A) and presence (B to D) of 0.5 M ethanol. The scan rates in panels A and D and panels B and C are 50 and 20 mV s^{-1}, respectively. The current densities are normalized by the Pd mass loaded (A, B, and D) and the ECSA values (C). The concentrations of citrate, AA, Na_2PdCl_4, and Au-NP seeds are 4.12 mM, 4.0 mM, 0.02 mM, and 1.5×10^{11}.

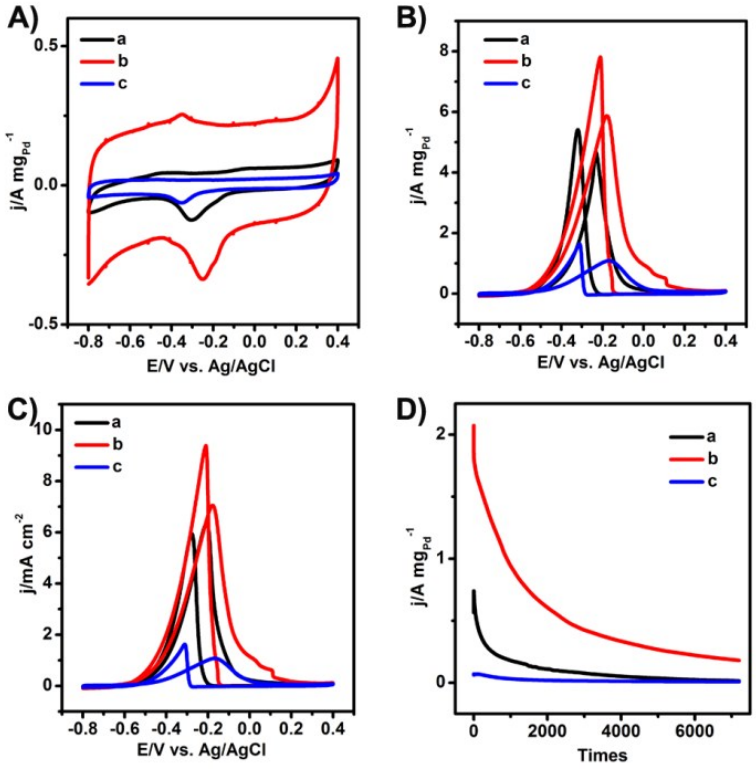

Fig. S15 Line charts of specific activities (A), ECSAs (B), and mass activities (C) of the corresponding C_mS $Au_x@Pd_{1-x}$ NPs without carbon supports (black column) and with carbon supports (red column), measured in 0.50 M KOH solution in the presence (A and C) and absence (B) of 0.5 M ethanol, respectively: C_6S $Au_{0.76}@Pd_{0.24}$ NPs and C_6S $Au_{0.76}@Pd_{0.24}$/C (a), $C_{12}S$ $Au_{0.85}@Pd_{0.15}$ NPs and $C_{12}S$ $Au_{0.85}@Pd_{0.15}$/C (b), $C_{19}S$ $Au_{0.91}@Pd_{0.09}$ NPs and $C_{19}S$ $Au_{0.91}@Pd_{0.09}$/C (c), $C_{30}S$ $Au_{0.95}@Pd_{0.05}$ NPs and $C_{30}S$ $Au_{0.95}@Pd_{0.05}$/C (d), $C_{57}S$ $Au_{0.97}@Pd_{0.03}$ NPs and $C_{57}S$ $Au_{0.97}@Pd_{0.03}$/C (e).

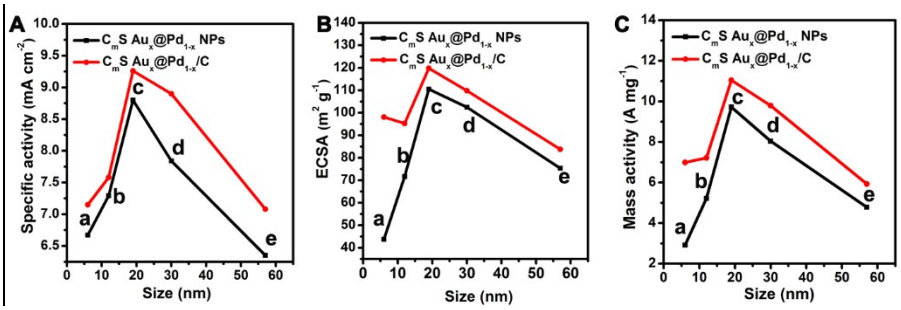

Fig. S16 TEM images (left) and HRTEM images (right) of as-prepared CTAC-C_mS Au@Pd NPs with various core sizes: CTAC-C_9S Au@Pd NPs (A), CTAC-C_{13}S Au@Pd NPs (B), CTAC-C_{20}S Au@Pd NPs (C), CTAC-C_{30}S Au@Pd NPs (D), and CTAC C_{55}S Au@Pd NPs (E), respectively.

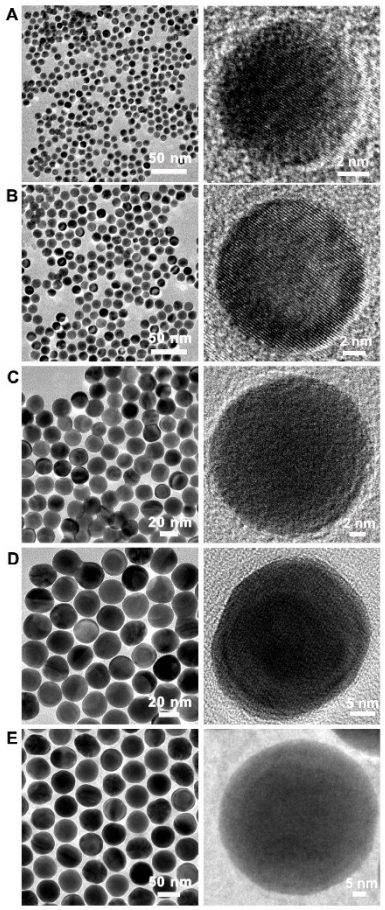

Fig. S17 CV curves (A to C) of the GCEs modified by CTAC-C_9S Au@Pd NPs (a, black curve), CTAC-C_{13}S Au@Pd NPs (b, red curve), CTAC-C_{20}S Au@Pd NPs (c, blue curve), CTAC-C_{30}S Au@Pd NPs (d, magenta curve), and CTAC C_{55}S Au@Pd NPs (e, olive curve), respectively, measured in 0.50 M KOH solution in the absence (A) and presence (B and C) of 0.5 M ethanol. The scan rates in panels A and panels B and C are 50 and 20 mV s^{-1}, respectively. The current densities are normalized by the Pd mass loaded (A and B) and the ECSA values (C), respectively.

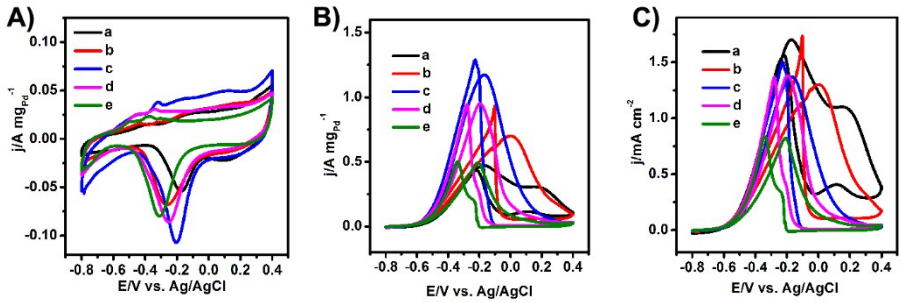

Fig. S18 Line charts of ECSAs (A), mass activities (B), and specific activities (C) of the corresponding CTAC-C_mS Au@Pd NPs measured in 0.50 M KOH solution in the absence (A) and presence (B and C) of 0.5 M ethanol, respectively: CTAC-C_9S Au@Pd NPs (a), CTAC-C_{13}S Au@Pd NPs (b), CTAC-C_{20}S Au@Pd NPs (c), CTAC-C_{30}S Au@Pd NPs (d), and CTAC C_{55}S Au@Pd NPs (e), respectively.

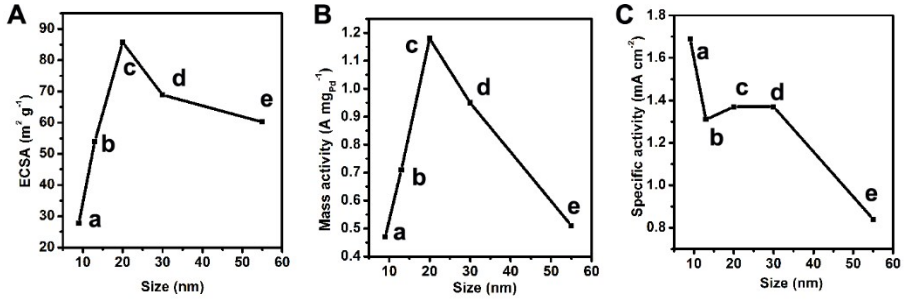

Fig. S19 TEM images of C_6S $Au_{0.76}@Pd_{0.24}$ NPs (a), $C_{12}SAu_{0.85}@Pd_{0.15}$ NPs (b), $C_{19}S$ $Au_{0.91}@Pd_{0.09}$ NPs (c), $C_{30}S$ $Au_{0.95}@Pd_{0.05}$ NPs (d), and $C_{57}S$ $Au_{0.97}@Pd_{0.03}$ NPs (e) after durability test.

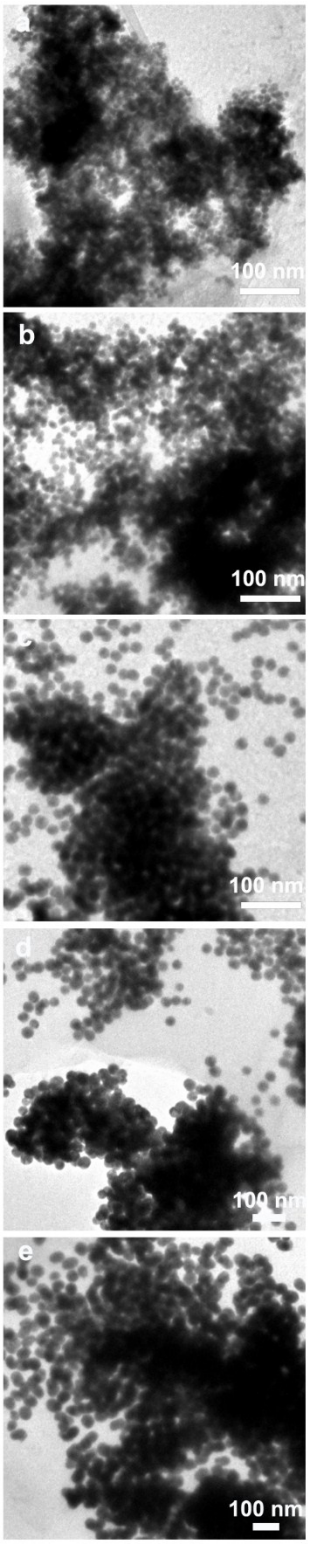

Fig. S20 TEM images (left) and HRTEM images (right) of C_6S $Au_{0.76}@Pd_{0.24}/C$ (A), $C_{12}S$ $Au_{0.85}@Pd_{0.15}/C$ (B), $C_{19}S$ $Au_{0.91}@Pd_{0.09}/C$ (C), $C_{30}S$ $Au_{0.95}@Pd_{0.05}/C$ (D), and $C_{57}S$ $Au_{0.97}@Pd_{0.023}/C$ (E) after durability test.

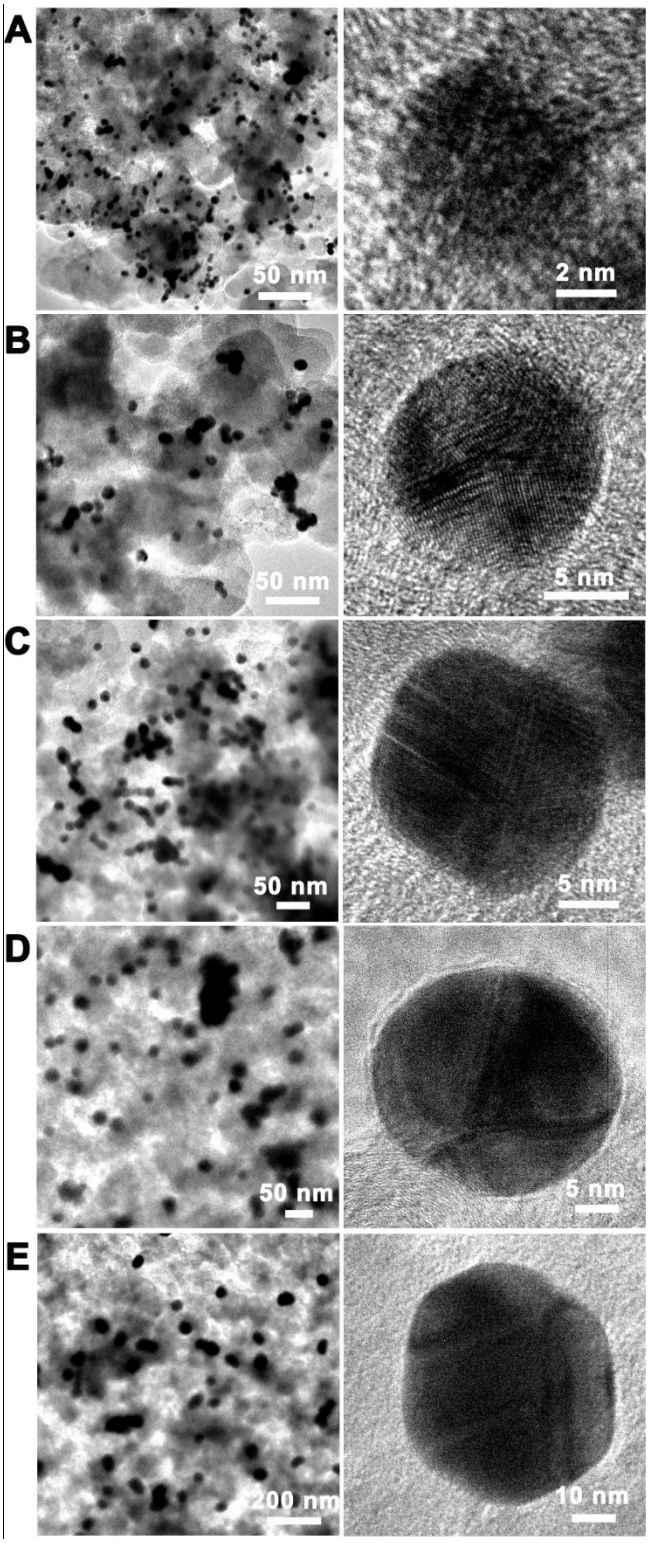

Fig. S21 The potential cycling stability (A) and mass activities during cycling test (B to F) of the GCEs modified by C_6S $Au_{0.76}@Pd_{0.24}$ NPs (a, black curve), $C_{12}S$ $Au_{0.85}@Pd_{0.15}$ NPs (b, red curve), $C_{19}S$ $Au_{0.91}@Pd_{0.09}$ NPs (c, blue curve), $C_{30}S$ $Au_{0.95}@Pd_{0.05}$ NPs (d, magenta curve), and $C_{57}S$ $Au_{0.97}@Pd_{0.03}$ NPs (e, olive curve), respectively, measured in 0.50 M KOH solution in the presence of 0.5 M ethanol: 100 cycle (B), 200 cycle (C), 300 cycle (D), 400 cycle (E), and 500 cycle (F).

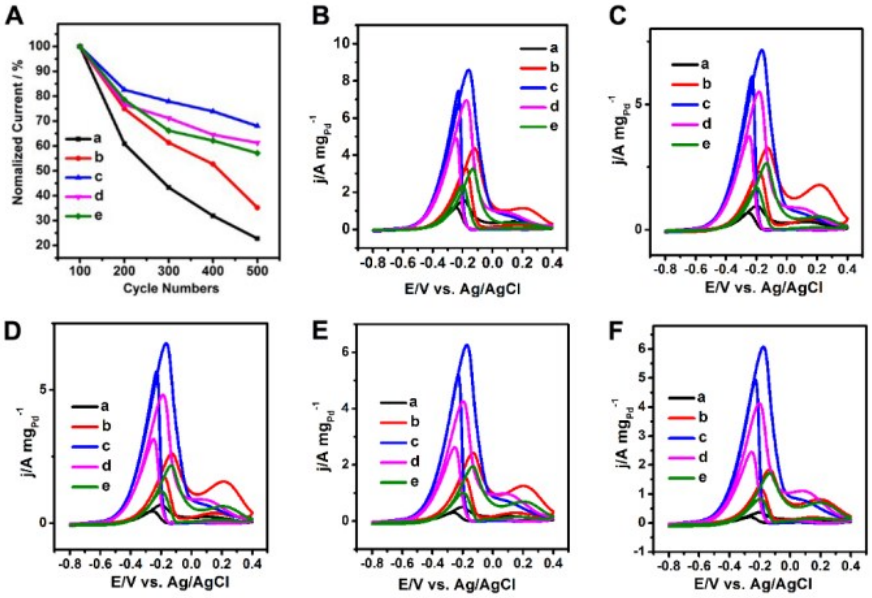

Fig. S22 The potential cycling stability (A) and mass activities during cycling test (B to F) of the GCEs modified by C_6S $Au_{0.76}@Pd_{0.24}/C$ (a, black curve), $C_{12}S$ $Au_{0.85}@Pd_{0.15}/C$ (b, red curve), $C_{19}S$ $Au_{0.91}@Pd_{0.09}/C$ (c, blue curve), $C_{30}S$ $Au_{0.95}@Pd_{0.05}/C$ (d, magenta curve), and $C_{57}S$ $Au_{0.97}@Pd_{0.03}/C$ (e, olive curve), respectively, measured in 0.50 M KOH solution in the presence of 0.5 M ethanol: 100 cycle (B), 200 cycle (C), 300 cycle (D), 400 cycle (E), and 500 cycle (F)

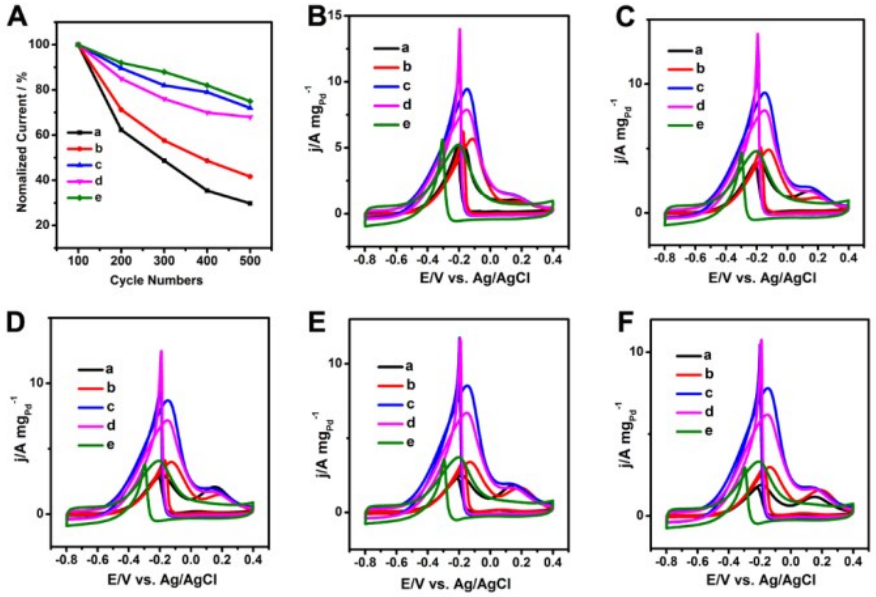

Fig. S23 Line charts of mass activities during cycling test (A to E) of the corresponding C_mS $Au_x@Pd_{1-x}$ NPs without carbon supports (black column) and with carbon supports (red column) measured in 0.50 M KOH solution in the presence of 0.5 M ethanol, respectively: 100 cycle (A), 200 cycle (B), 300 cycle (C), 400 cycle (D), and 500 cycle (E). These samples were C_6S $Au_{0.76}@Pd_{0.24}$ NPs and C_6S $Au_{0.76}@Pd_{0.24}$/C (a), $C_{12}S$ $Au_{0.85}@Pd_{0.15}$ NPs and $C_{12}S$ $Au_{0.85}@Pd_{0.15}$/C (b), $C_{19}S$ $Au_{0.91}@Pd_{0.09}$ NPs and $C_{19}S$ $Au_{0.91}@Pd_{0.09}$/C (c), $C_{30}S$ $Au_{0.95}@Pd_{0.05}$ NPs and $C_{30}S$ $Au_{0.95}@Pd_{0.05}$/C (d), $C_{57}S$ $Au_{0.97}@Pd_{0.03}$ NPs and $C_{57}S$ $Au_{0.97}@Pd_{0.03}$/C (e), respectively.

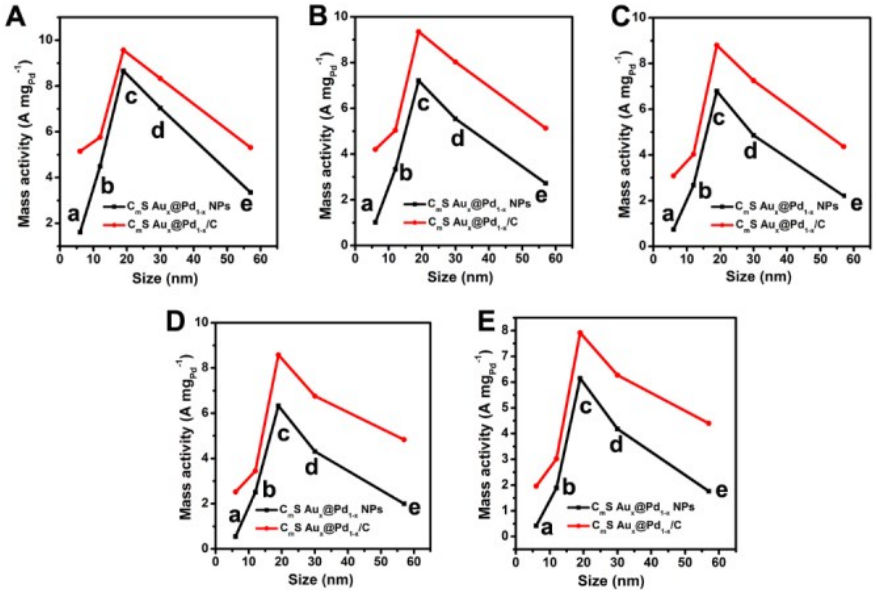

Table S1. The detailed for synthesis of Au NPs with size range from 6 nm to 57 nm by citrate reduction of $HAuCl_4$

Size (nm)	Citrate (mM)	$HAuCl_4$ (mM)	$AgNO_3$ (μM)	Premixed time (min)
6	1.72	0.25	5.05	16
12	1.03	0.25	5.05	5
19	1.03	0.25	5.05	--
30	0.52	0.375	5.05	4.5
57	0.17	0.25	10.1	--

Table S2. Summary of the concentrations of AA, ECSAs, mass activity, and specific activity of the GCEs modified by different AA-to-Pd molar ratio of $C_{19}S$ $Au_{0.91}@Pd_{0.09}$ NPs with respect to ethanol oxidation in 0.50 M KOH solution containing 0.50 M ethanol.

[AA] (mM)	Molar ratio of AA-to-Pd	ECSA ($m^2\ g^{-1}$)	Mass activity ($A\ mg^{-1}$)	Specific activity ($mA\ cm^{-2}$)
0	0	11.6	0.3	2.6
0.04	2:1	25.4	0.9	3.5
0.40	20:1	58.3	4.8	8.2
2	100:1	75.3	7.1	9.4
4	200:1	108.2	9.7	8.9
8	400:1	96.4	8.8	9.1

Table S3. Summary of the recipes for synthesizing $C_mS\ Au_x@Pd_{1-x}$ NPs with various core sizes and about one Pd atomic layer. The concentrations of citrate, Na_2PdCl_4, and AA are 4.12, 0.02, and 4 mM, respectively.

Sample	Sample image	Core size (nm)	Total number of Au-NP seeds	S_{total} (10^{-3} m^2)
$C_6S\ Au_{0.76}@Pd_{0.24}$ NPs	Figure 1A	6.1	1.3×10^{13}	1.5
$C_{12}SAu_{0.85}@Pd_{0.15}$ NPs	Figure 1B	12.1	3.3×10^{12}	1.5
$C_{19}S\ Au_{0.91}@Pd_{0.09}$ NPs	Figure 1C	19.3	1.3×10^{12}	1.5
$C_{30}S\ Au_{0.95}@Pd_{0.05}$ NPs	Figure 1D	30.4	5.3×10^{11}	1.5
$C_{57}S\ Au_{0.97}@Pd_{0.03}$ NPs	Figure 1E	57.2	1.5×10^{11}	1.5

Table S4. Summary of the Pd 3d, Au 4f binding energies of pure Pd NPs, spherical pure Au NPs and $C_{19}S$ $Au_{0.91}$@$Pd_{0.09}$ NPs.

	Pd $3d_{5/2}$ peak(eV)	Pd $3d_{3/2}$ peak(eV)	ΔPd $3d_{5/2}$ (eV)	Au $4f_{7/2}$ peak(eV)	Au $4f_{5/2}$ peak(eV)	ΔAu $4f_{7/2}$ (eV)
Pd NPs	335.0	340.2	0	--	--	--
Au NPs	--	--	--	83.7	87.4	0
$C_{19}SAu_{0.91}$@ $Pd_{0.09}$ NPs	335.3	340.5	+ 0.3	83.4	87.1	- 0.3

Table S5. Summary of ECSAs, mass activities, and specific activities of the GCEs modified by CTAC-C_9S Au@Pd NPs, CTAC-C_{13}S Au@Pd NPs, CTAC-C_{20}S Au@Pd NPs, CTAC-C_{30}S Au@Pd NPs, and CTAC C_{55}S Au@Pd NPs with respect to ethanol oxidation in 0.50 M KOH solution containing 0.50 M ethanol.

Sample	ECSA (m^2 g^{-1})	Mass activity (A mg^{-1})	Specific activity (mA cm^{-2})
CTAC-C_9S Au@Pd NPs	27.8	0.47	1.69
CTAC-C_{13}SAu@Pd NPs	54.0	0.71	1.31
CTAC-C_{20}S Au@Pd NPs	85.7	1.18	1.37
CTAC-C_{30}S Au@Pd NPs	68.9	0.95	1.37
CTAC-C_{55}S Au@Pd NPs	60.2	0.51	0.84